Crystallisation of a zirconium-based glaze for ceramic tile coatings

M. Romero[a,*], J. Ma. Rincón[a], A. Acosta[b]

[a]*Laboratory of Glass-Ceramic Materials, Instituto Eduardo Torroja de Ciencias de la Construcción, CSIC, Serrano Galvache s/n, 28033, Madrid, Spain*
[b]*Department of Applied Mineralogy, Universidad de Castilla-La Mancha, Facultad de CC. Químicas, Avda. Camilo José Cela 10, 13071, Ciudad Real, Spain*

Abstract

The effect of iron oxide content on the crystallisation of a zirconium-based glass-ceramic glaze was investigated using a glass-ceramic "white of zirconium" frit and a granite waste glass. Measurements by X-ray diffraction (XRD) combined with scanning electron microscopy (SEM) and EDX microanalysis showed that Fe_2O_3 gives rise to the crystallisation of an iron-zinc ferrite, which is acting as nucleating agent of feather-like crystals of pyroxene while granite frit enhances the partial dissolution of zircon into the glassy phase, which is sharply increased for granite frit additions greater than 50%.
© 2003 Elsevier Science Ltd. All rights reserved.

1. Introduction

Glazed ceramic tiles are the most common building material for floor and wall covering in Mediterranean countries. Glazed tiles are produced from frits (glasses quenched in water), which are mixed with water and organic additives to yield glaze slips. These slips are applied on the surface of green tiles and after a drying step, they are subjected to a single or double-firing process. There are a wide variety of frits, which have different characteristics such as fusibility, viscosity, gloss and opacity. Amongst commercial frits, those containing zircon ($ZrO_2·SiO_2$) and zirconia (ZrO_2) are of great interest. $ZrSiO_4$ gives rise to opaque frits, which are commonly designated as "white of zirconium". This type of frits, which are glossy, opaque, viscous and with low fusibility, are composed by SiO_2 (50–60 wt.%), ZrO_2 (8–14 wt.%) and fluxing elements such as Na_2O, K_2O, PbO and B_2O_3 (20–25 wt.%) as major components and stabilizing elements such as ZnO, Al_2O_3, CaO, BaO, MgO as minor components (7–9 wt.% maximum). $ZrSiO_4$ was proved to enhance opacity,

especially in the presence of ZnO providing that SiO_2/Al_2O_3 molar ratio is equal to 10.[1,2]

Glass-ceramics, which are polycrystalline materials comprised of crystalline and glassy phases, have become established in a wide range of technical and technological applications.[3,4] The glass-ceramic process involves the controlled devitrification of a glass in order to provide a homogeneous microcrystalline structure. To achieve this, it has usually been necessary to include a nucleating agent, such as TiO_2 or Fe_2O_3, in the glass which will provide the nuclei for subsequent crystal growth, or influence the structural reorganisation in such a manner that many crystals grow.[3,5]

Opaque glazes are composed of a considerable amount of finely dispersed opacifying crystals in a glassy matrix. Thus, zirconium glazes could be considered as glass-ceramic glazes. The properties, microchemistry and microstructure of zirconium glazes has been studied in previous works.[6–8] However, to our knowledge, no data concerning the influence of a nucleating agent on the crystallisation of zirconium glazes are available in the literature.

The aim of the present work, which is part of the wider study on glassy and glass-ceramic glazes from granite wastes, is to study the effect of Fe_2O_3 on crystallisation behaviour of a "white of zirconium" frit.

---

* Corresponding author. Tel. +34-91-302-0440; fax: +34-91-302-0700.

E-mail address: nromero@ietcc.csic.es (M. Romero).

2. Materials and methods

The chemical composition (determined by using inductively coupled plasma emission spectroscopy, ICP) of a "white of zirconium" frit (designated WZ frit) which was supplied by Fritta S.L., is given in Table 1. An iron rich waste originated by a Spanish granite plant was used to prepare an iron glass, which were melted in air, in a silica–alumina crucible, in a laboratory electric furnace at 1450 °C for 1 h. The molten material was quenched by pouring into water to obtain a frit. No visible corrosion or chemical attack of the silica-alumina crucible by the melt was observed. The chemical composition of granite frit is also given in Table 1. In the Table, Fe_2O_3 represents the total amount of $FeO + Fe_2O_3$.

Both WZ and granite frits were found to be glassy as determined by X-ray diffraction (XRD) analysis in a Philips X'PERT MPD diffractometer using CuK_α radiation. The frits were crushed and sieved to < 65 μm particle size. Different frits mixtures were prepared from WZ and granite frits as given in Table 2. The iron content of those mixtures is also shown in Table 2. As noted, the Fe_2O_3 content ranges from 0 wt.% in 100Z mixture, which is only composed by zircon frit, to near 9% for 50Z mixture, which is prepared with addition of a 50% of granite frit.

Frits mixtures were mixed with water and organic additives (tripolyphosphate and carbosymethylcellulose)

Table 1
Chemical composition (by ICP method) of zircon and granite frits

	Zircon frit	Granite frit
SiO_2	53.89	55.24
Al_2O_3	4.46	12.42
Fe_2O_3	0.00	17.79
ZrO_2	12.93	0.00
CaO	9.42	5.89
MgO	2.03	1.83
MnO	0.00	0.16
BaO	0.00	0.06
ZnO	12.96	0.11
Na_2O	0.58	2.64
K_2O	3.73	3.34
TiO_2	0.00	0.35
P_2O_5	0.00	0.16

Table 2
Original frit mixtures prepared from zircon and granite frits

Frit mixture	Zircon frit (% wt)	Granite frit (% wt)	Fe_2O_3 content (% wt)
100Z	100	0	0.00
90Z	90	10	1.78
70Z	70	30	5.34
50Z	50	50	8.89

to obtain a slip, which was poured onto 80×80 mm² fired ceramic tiles to produce a≈500 μm coating. The coated tiles were dried in air for 24 h and fired at 1120 °C for 15 min with heating and cooling rates of 50 °C/min. After cooling to room temperature, glaze tiles showed homogeneous surface. Glaze defects as bubbles or crazing were not detectable. The crystalline phases developed in the glaze after heat treatment were determined by XRD.

Scanning electron microscopy (SEM) of etched samples (2% HF for 1 min) was used to examine the microstructure of the glass-ceramics. SEM observations were carried out in a Philips scanning electron microscope at an acceleration voltage of 20 kV and energy dispersive X-ray (EDX) analysis with a solid state detector (Be window).

3. Results and discussion

Fig. 1 shows the X-ray spectra collected from the surface of glazed tiles. The XRD pattern of sample 100Z (Fig. 1a), which is prepared without addition of the granite frit, shows that ZW frit gives rise to a glass-ceramic glaze comprised by diopside, $Ca(Mg, Al)(Si, Al)_2O_6$ (JCPDS file No. 41-1870) and zircon, $ZrSiO_4$. It should be noted that the (h00) reflections of diopside in 100Z glaze are strongly increased in comparison with the XRD pattern shown in Fig. 1, which could be attributed to the alignment of basal planes of diopside crystals parallel to the glaze surface. Diopside, which gives rise to high erosion and corrosion resistant tiles, is one of the most commonly crystalline phase of ceramic glazes but to the authors knowledge, the orientation of diopside crystals in ceramic glazes has not been described before. As for $ZrSiO_4$, all hkl reflections can be observed in Fig. 1.

The microstructure of 100Z glaze is presented in Fig. 2. The surface of the glaze shows a high degree of crystallisation (Fig. 2a) and the microstructure is composed of irregular size and shape crystals, which correspond to diopside phase, and very fine needle-like crystals of $ZrSiO_4$ (Fig. 2b), which are homogeneously dispersed on the whole sample.

Table 3 gives the chemical composition of 100Z glaze and of the different phases as analysed by EDX. The residual glassy phase is enriched in SiO_2, Al_2O_3 and alkaline oxides while the CaO and MgO content is greater in diopside crystals. As for zircon crystals, ZrO_2 and SiO_2 are the main components although EDX analysis also shows a high Al_2O_3, MO and M_2O contents; this is a consequence of the small size of $ZrSiO_4$ needles, which is down to the analytical resolution of the SEM/EDX system (1 μm).

Fig. 3 shows the microstructure of 90Z glaze prepared with addition of a 10% of granite frit. As in 100Z sample,

Fig. 1. XRD patterns from 100Z, 90Z, 70Z, 50Z and 30Z glazes. Peaks shown are for diopside (D), zircon (Z) and iron-zinc ferrite (F).

the surface of 90Z glaze is fully crystallised but new crystalline regions with high white contrast appears (Fig. 3a). These crystalline regions, which show irregular shape and size, are comprised by small rounded crystals whose average diameter is 0.90 μm (Fig. 3b). Table 4 collects the EDX analyses carried out on 90D glaze. As noted, rounded crystals show greater Fe_2O_3 and ZnO content when compared with the average composition, thus this crystalline phase could be identified as a ferrite

such as magnetite ($FeO \cdot Fe_2O_3$) or franklinite ($ZnO \cdot Fe_2O_3$) or even a mixture of both ferrites, which have also been identified in a former investigation on the influence of iron oxide on the crystallisation of diopside glazes.[9] EDX analysis also shows a high CaO and Na_2O contents; the presence of CaO is likely owing to the ionic substitution of Zn^{2+} and Fe^{2+} by Ca^{2+} ions in the crystalline structure of the ferritic phase. In fact, this type of ionic substitutions, which are usual in pyroxenic

Fig. 2. SEM observations on the surface of 100Z glass-ceramic glaze.

Table 3
Chemical composition of 100Z glaze and of the different phases as analysed by EDX spectrometry

	SiO_2	Al_2O_3	CaO	MgO	ZnO	ZrO_2	M_2O[a]
Diopside crystals	57.60	4.02	16.84	15.71	4.37	0.00	1.46
Zircon crystals	34.19	5.98	4.92	1.91	2.61	46.93	3.46
Glassy phase	64.34	7.55	6.95	4.94	3.62	3.58	9.01

[a] $= Na_2O + K_2O$.

phases, have been also detected in ferrites.[10] More difficulty involves to explain the presence of Na^+ ions in the EDX analysis. Because of the low SiO_2 content, it does not seem likely the crystallisation of a sodium based pyroxenic phase such as aegirine or jadeite and hence, the high Na_2O content can only be ascribed to an effect of X-ray channeling owing to the nearness between the energies of Na K_α (1.04 eV) and Zn L_α (1.01 eV) peaks, which causes an overvaluation of Na_2O at the expense of ZnO content. In fact, abnormal increase of EDX lines, which is owing to an orientation effect, has been previously described in the literature in cubic structures such as garnets and ferrites,[11,12] as well as in SiC-based materials with cubic β-SiC phase.[13] Because of its low percentage in the glaze (< 2%), the iron-zinc ferrite is not still detectable in the XRD pattern of 90D glaze (Fig. 1b). As noted in Fig. 3c, the ferrite is acting as nucleating agent of a new phase consisting of feather-like crystals.
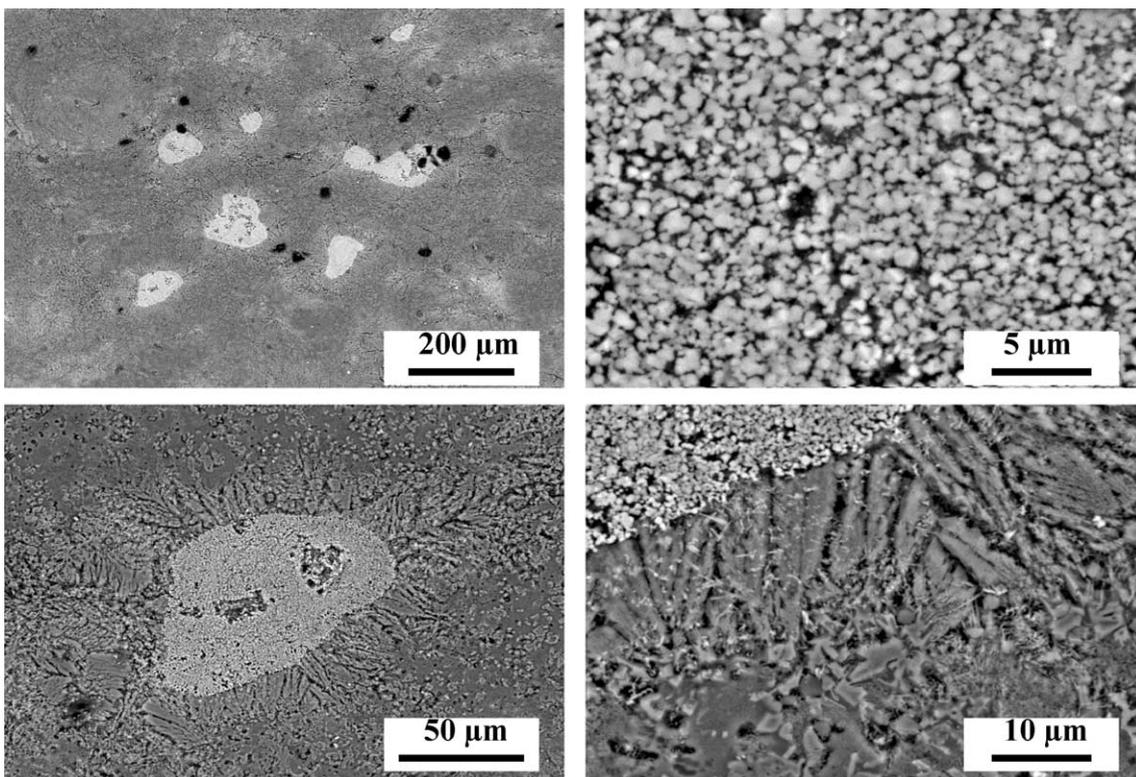
Fig. 3. SEM observations on the surface of 90Z glass-ceramic glaze.

Table 4
Chemical composition of 90Z glaze and of the different phases as analysed by EDX spectrometry

	SiO_2	Al_2O_3	Fe_2O_3	CaO	MgO	ZnO	ZrO_2	Na_2O	K_2O
Average	58.63	7.60	1.91	7.14	2.69	7.52	4.66	6.28	3.55
Rounded crystals	6.09	13.78	26.08	12.60	4.39	12.40	0.47	23.25	0.94
Feather like crystals	61.45	9.10	3.52	8.78	4.73	2.80	0.00	6.39	3.23
Diopside crystals	54.13	3.03	1.53	16.91	13.23	4.32	0.00	5.65	1.20

EDX analyses carried out on those crystals along with their morphology and the absence of new diffraction lines in the XRD diffractogram of 90D glaze when compared with 100D glaze allow identify this phase as a half member of the pyroxene group, which undergoes a wide variety of ionic substitutions.[14,15] As for oriented diopside, this phase also crystallises in 90D sample but in lower content that in 100D and hence the intensity of (h00) reflections decreases.

ZrSiO$_4$ needles persist homogeneously dispersed in 90Z glaze although SEM observations shows a slight decrease in their volume fraction also detectable in the XRD pattern (Fig. 1b). It can be noted from Fig. 1b–e that zircon crystallisation decreases as the percentage of granite frit increases. The mixed (312) reflection of zircon (JCPDS file No. 6-266), with a d-spacing of 1.712 nm, is normally used for quantitative crystallisation studies.[8,16] This peak is chosen because of its location above the amorphous hump and because mixed peaks are less susceptible to orientation effects. Although for quantitative purposes a base calibration is required, the change in the intensity of (312) reflection can get a

qualitative information on zircon crystallisation. In this way, the intensity of (312) reflection of zircon, as a function of the amount of granite frit added is plotted in Fig. 4. It can be noted that the intensity of (312) reflection decreases up to a minimum, at 30% of granite addition, from which stars to increase. It seems to be that great additions of granite frit enhance zircon recrystallisation but this is a fictitious effect owing to an increase in the crystallisation of the zinc-iron ferrite as explained below. The (422) reflection of the ferrite, with a d-spacing of 1.723, overlaps with (312) reflection of zircon and causes the mentioned result. Based on the above, the (200) reflection of zircon, with a d-spacing of 3.302 nm, appears more adequate for the qualitative evaluation of zircon crystallisation. The intensity of (200) reflection, as a function of the amount of granite frit added, which is also plotted in Fig. 4, depicts a linear decrease of zircon crystallisation as granite frit increases. A better way to asses the effect of granite frit on zircon crystallisation is to define the relative intensity (I_r) of a deflection peak as follows:
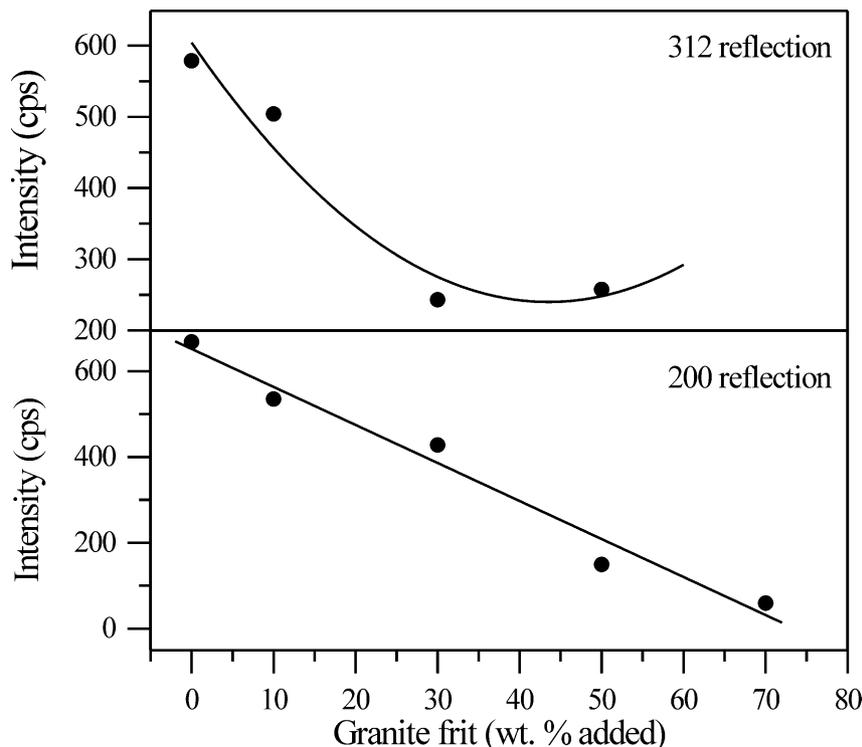
Fig. 4. Intensity of (312) reflection of zircon, as a function of the amount of granite frit added.

$$I_{r(hkl)} = \frac{I_{(hkl)}}{I_{WZ(hkl)}} \times 100$$

being $I_{WZ(hkl)}$ the intensity of (hkl) deflection in 100Z glaze, which is formulated without granite frit addition. Fig. 5 shows the plot of the relative intensity (I_r) of the (200) reflection of zircon versus the content (wt.%) of WZ frit in the glazes. In all cases I_r is below to the line of full zircon crystallisation (dotted line) pointing out that granite frit enhances the partial dissolution of zircon into the glassy phase, which is sharply increased for granite frit additions greater than 50%.

Fig. 6 shows the microstructure of 70Z glaze, which is prepared with the addition of a 30% of granite frit. The iron-zinc ferrite begins to be detectable in the X-ray spectra collected from this glaze (Fig. 1c) and in the SEM observation (Fig. 6a), which show greater volume percentage of crystalline regions with high secondary electron emission. The average diameter of the ferrite crystals (Fig. 6b) is 0.62 μm, which is slightly lower than that showed in 90Z glaze (0.90 μm). It can be noted from Fig. 6b that feather-like crystals of pyroxene rise above initial diopside crystals, which is also perceptible in Fig. 1c.

Finally, Fig. 1d–e. shows that the increase of granite frit content up to 70% leads to a glass-ceramic glaze with lower content of diopside and zircon, the iron-zinc ferrite being the main crystalline phase.
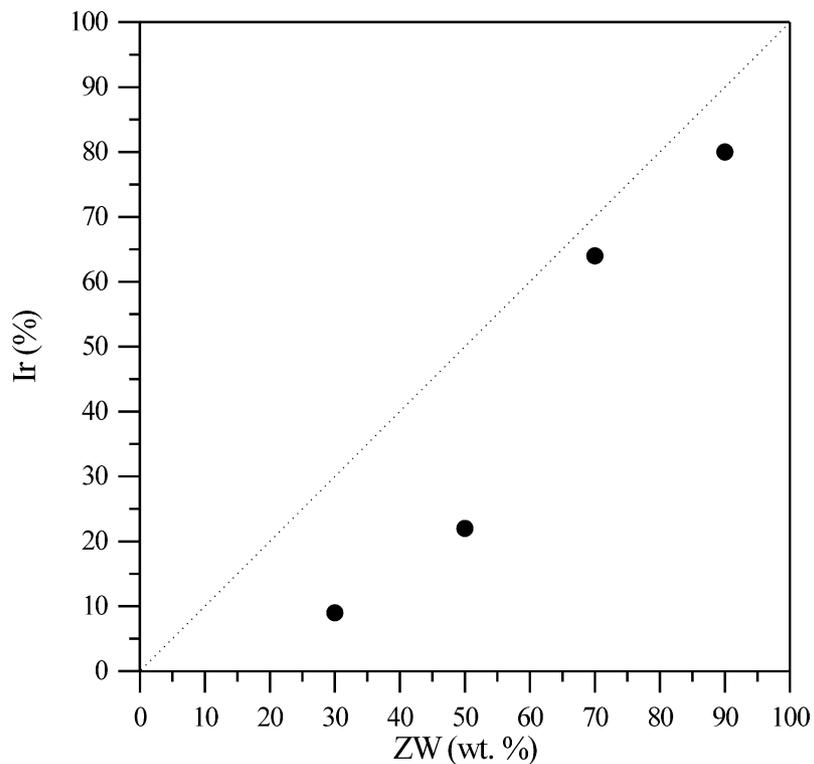
Fig. 5. Relative intensity (I_r) of (200) reflection of zircon versus the content (wt.%) of WZ frit in the glazes.
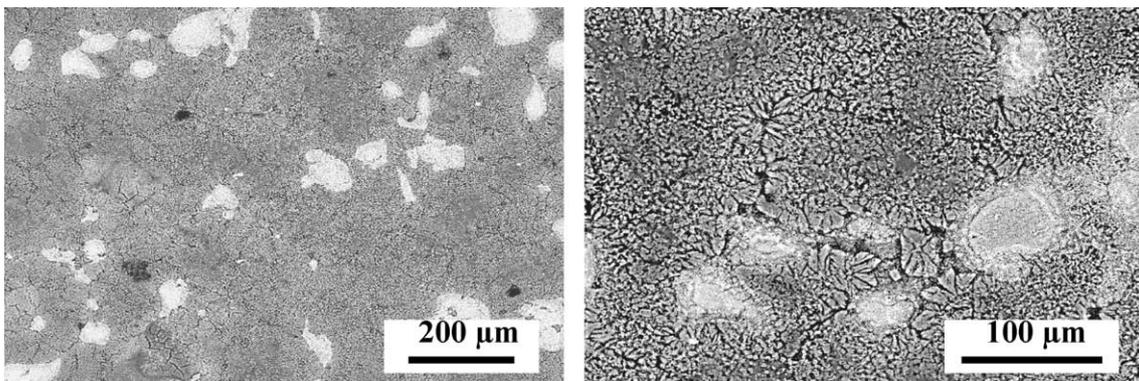
Fig. 6. SEM observations on the surface of 70Z glass-ceramic glaze.

4. Conclusion

The influence of Fe_2O_3 as nucleating agent on the crystallisation of a zirconium-based glass-ceramic glaze has been established. XRD patterns and SEM observations on the surface of glass-ceramic glazes showed that WZ ("white of zirconium") original frit gives rise to a glass-ceramic glaze comprised by irregular size and shape crystals of diopside, $Ca(Mg, Al)(Si, Al)_2O_6$, and very fine needle-like crystals of zircon, $ZrSiO_4$. The basal planes of diopside crystals are aligned parallel to the glaze surface.

The inclusion of Fe_2O_3 to the glaze by means of additions of a granite glassy frit to WZ frit gives rise to the crystallisation of small rounded crystals of an iron-zinc ferrite, which are acting as nucleating agent of a new phase consisting of feather-like crystals of pyroxene.

Zircon crystallisation decreases as the percentage of granite frit, and hence Fe_2O_3 content, increases. The variation of the relative intensity (I_r) of the (200) reflection of zircon had shown that granite frit enhances the partial dissolution of zircon into the glassy phase, which is sharply increased for granite frit additions greater than 50%.

Acknowledgements

References

1. Parmalee, C. W., *Ceramic Glazes*. Cahners Books, Boston, 1973.
2. Sainz, I. G., Physical-chemical characteristics of ceramic glazes and their influence on quality of floor and wall tiles. *Tile Brick Int.*, 1990, **6**, 21.
3. Partridge, G., An overview of glass ceramics. Part 1. Development and principal bulk applications. *Glass. Technol.*, 1994, **35**, 116–127.
4. Manfredini, T., Pellacani, G. C. and Rincón, J.Ma., *Glass-Ceramic Materials. Fundamentals and Applications*. Mucchi Editore, Modena, 1997.
5. Rincón, J.Ma., Principles of nucleation and controlled crystallization of glasses. *Polym-Plast. Technol. Eng.*, 1992, **31**, 309–357.
6. El-Defrawi, S. A. and Abd El-Fattah, W. I., Pinholes and introduction of albite in double firing zircon-glazed tiles. *Silicates Industriels*, 1993, **58**, 31.
7. El-Defrawi, S. A., Serry, M. A., Abd El-Fattah, W. I. and Weisweiler, W., Microchemistry and microstructure of some opaque glaze/tile interfaces in relation to their physical properties. *Ceramics International*, 1995, **21**, 69–75.
8. Castilone, R. J., Sriram, D., Carty, W. M. and Snyder, R. L., Crystallization of zircon in stoneware glazes. *J. Am. Ceram. Soc.*, 1999, **24**, 2819–2824.
9. Romero, M., Rincón, J.Ma. and Acosta, A., Effect of iron oxide content on the crystallisation of a diopside glass-ceramic glaze. *J. Eur. Ceram. Soc.*, 2002, **22**, 883–890.
10. Gerardin, R., Bonazebi, A., Millon, E., Brice, J. F., Evrard, O. and Sanchez, J. O., Magnetite doped with lime: substitution of iron by calcium in tetrahedral site. *J. Solid State Chem.*, 1989, **78**, 154–163.
11. Khrisnan, K.M., *Atomic Site and Species Determination Using Channeling and Related Effects in AEM. Ultramicroscopy on Limits of Submicron Spectroscopy*, ed. Hren and Kersker, 1987.
12. Spence, J. C. H., Reese, N., Yamamoto, N. and Kurizki, G., Coherent Bremmstrahlung peaks in x-ray microanalysis spectra. *Phil. Mag. B*, 1983, **48**, L39–L43.
13. Rincón, J.Ma., Electron microscopy and EDX microanalysis of Si_3N_4, AlN and SiC powders, their sintered products and some SiAlON glass-ceramics. *J. Mat. Education*, 1988, **10**, 647–672.
14. Deer, W. A., Howie, R. A. and Zussman, J., *Rock Forming Minerals, Vol. 2*. Longman, London, 1963.
15. Romero, M., Rincón, J.Ma., Rawlings, R. D. and Boccaccini, A. R., Use of vitrified urban incinerator waste as raw material for production of sintered glass-ceramics. *Materials Research Bulletin*, 2001, **36**, 383–395.
16. Earl, D. A. and Clark, D. E., Effects of glass frit oxides on crystallization and zircon pigment dissolution in whiteware coatings. *J. Am. Ceram. Soc.*, 2000, **83**, 2170–2176.